Elastic Scattering of He^3 at 20 MeV*

RAYMOND W. KLINGENSMITH†
Battelle Memorial Institute, Columbus, Ohio

AND

HERSHEL J. HAUSMAN AND WILLIAM D. PLOUGHE
The Ohio State University, Columbus, Ohio

(Received 9 September 1963; revised manuscript received 2 March 1964)

Absolute differential elastic scattering cross sections were measured for the scattering of 20-MeV He^3 particles from V, Ni, Cu, Rh, Sn^{118}, Sm, Yb, and Pb. Where practical the measurements were made at laboratory angles extending from 20 to 170 deg. The diffraction-like oscillations exhibited by the elastic-to-Coulomb cross-section ratios are not highly pronounced. A preliminary optical-model analysis was carried out using the HUNTER automatic search code of Drisko and Bassel. A Woods-Saxon potential with Thomas-type spin-orbit coupling was considered. Reasonable fits to the data were obtained.

INTRODUCTION

ABSOLUTE differential elastic scattering cross sections were measured at 20 MeV for V, Ni, Cu, Rh, Sn^{118}, Sm, Yb, and Pb from 20 to 170 deg (laboratory angles). The measurements were made to provide He^3 data at this energy over a wide range of the periodic table. It is expected that these data will complement those at both higher and lower energies.[1–3] As expected, the elastic-to-Coulomb cross-section ratio was found to deviate from unity but the diffraction-like oscillations are not highly pronounced. In addition to the listed elements, measurements were carried out for yttrium and bismuth. However, due to experimental difficulties, these data have not yet been analyzed. A preliminary optical-model analysis of the data was carried out. The intent of the analysis is to indicate the general applicability of the model to the data and to obtain reasonable model parameters.

EXPERIMENTAL APPARATUS AND TECHNIQUES

Doubly ionized He^3 ions were accelerated to an energy of 20.0 ± 0.2 MeV in The Ohio State University cyclotron. The beam was extracted from the cyclotron chamber and focused by a pair of quadrupole magnets and a 15-deg beam-analyzing magnet onto a target located at the center of a 22-in.-diam scattering chamber. Within the scattering chamber, a rotating platform, driven by a remotely controlled variable-speed dc motor, carried the scattered-particle detector and collimator through an angular span of 170 deg (laboratory). The angular position of the detector was tracked by a pair of Selsyn motors and measured to an absolute accuracy of ±0.1 deg.

TABLE I. Target properties.

Material	Average thickness (mg/cm^2)	Isotopic abundance	Displacement correction factor
V	8.3	Natural	1.00
Ni	1.3	Natural	1.19
Cu	2.4	Natural	1.24
Rh	1.2	Natural	1.00
Sn	2.8	97% Sn^{118}	1.07
Sm	3.6	Natural	0.95
Yb	1.4	Natural	0.98
Pb	0.3	Natural	1.28

A movable target holder capable of supporting three mounted targets was located at the center of the scattering chamber. The holder could be moved vertically and rotated about its vertical axis without breaking the chamber vacuum. An external scale indicated the position of the holder with respect to each mode of movement. Positioning of the holder was done manually and was independent of all other movements within the chamber.

The beam collimator consisted of a tapered brass tube 8.1 in. long with aluminum defining apertures press fitted into the ends. The final aperture was 0.064 in. in diameter and was located 3 in. from the center of the chamber. In addition, a slightly larger aperture at the center of the tube reduced internal beam scatter. The resulting beam spot, as it appears at the target, was a well defined circle with a diameter of approximately 0.1 in. Maximum beam current on target was 0.3 μA.

The targets consisted of thin foils mounted in brass frames designed to fit into the holder in the scattering chamber. Properties of the targets used are given in Table I. Thickness measurements were considered accurate only to $\pm10\%$. The lead target was mounted on a 0.02 mg/cm^2 aluminum backing. All other targets were self-supporting.

A gold-silicon surface barrier solid-state detector was used as the scattered-particle detector. The resolution of the detector was measured and found to be 37 keV,

* This work was supported in part by the National Science Foundation.

† This article is based on a portion of a doctoral thesis submitted by R. W. Klingensmith to the faculty of The Ohio State University.

[1] G. W. Greenlees and R. C. Rowe, Nucl. Phys. **15**, 687 (1960).

[2] G. W. Greenlees, J. S. Lilley, and R. C. Rowe, Nucl. Phys. **24**, 334 (1961).

[3] H. E. Wegner, Los Alamos Scientific Laboratory, Los Alamos, New Mexico (to be published).

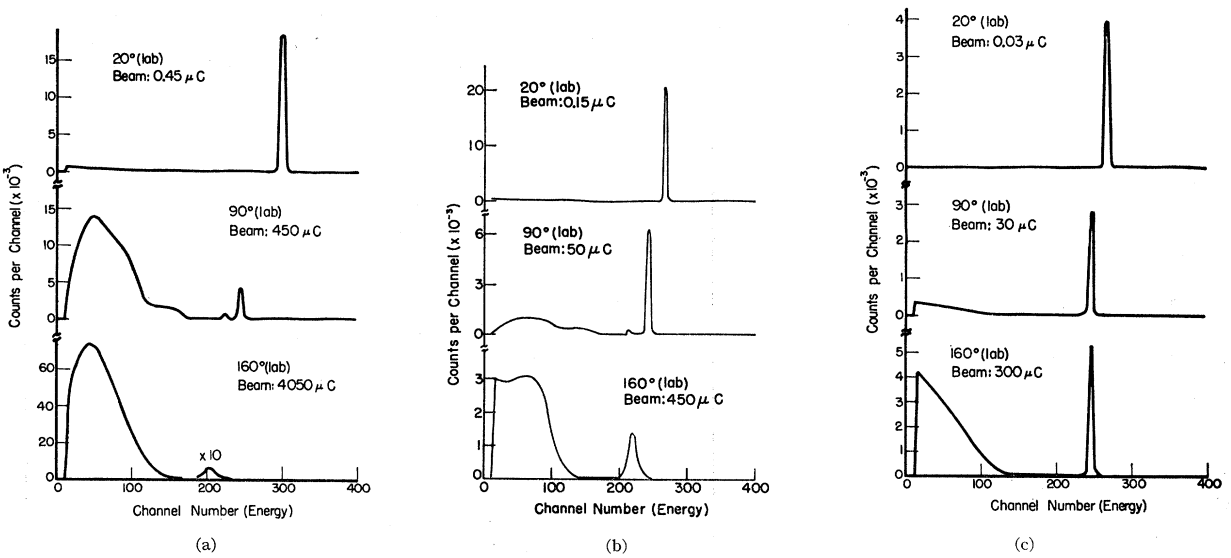

FIG. 1. Spectra of 20-MeV He^3 scattered by (a) nickel, (b) tin^{118}, and (c) lead.

FWHM for 5.30-MeV alpha particles. A dc bias voltage of 120 V applied to the detector created a depletion region 340 μ in depth. This depth was sufficient to stop 25-MeV He^3 particles and proved adequate for this experiment.

A solid angle of 3.42×10^{-4} sr was subtended at the detector by means of a collimator consisting of a 0.125-in.-diam defining aperture located 5.98 in. from the target. The half-angle thus subtended at the detector was 0.6 deg. Measurements of this solid angle over the range 0 to 170 deg (laboratory) indicated its value to be constant to within 1%.

A closed-loop gas handling system was provided in order to reduce to a minimum the inventory of He^3 gas necessary. The system was patterned after the Los Alamos system[4] and consisted essentially of a main recirculating loop and a series of smaller loops which transferred the gas to a storage tank. Only minor modification of the pumps was necessary to provide adequate integrity for the He^3 application. When the cyclotron was not in use or when other ions were being accelerated, the He^3 gas was pumped out of the recirculating loop and into the storage tank.

EXPERIMENTAL RESULTS

The data accumulated in this experiment consisted of charged-particle spectra taken at 5-deg intervals over a laboratory angular range from 20 to 170 deg. The counting times were varied such that a nominal total of ten thousand elastic events were recorded. The extreme values of accumulated charge varied between 4.5×10^{-9} C and 4.5×10^{-4} C depending upon target thickness and scattering angle. As a result, the time elapsed during a counting cycle varied from a few minutes to several hours. To avoid pulse pile-up in the amplifier, the beam intensity was maintained such that the total detector count rate did not exceed one-thousand counts per second. The current integrator was periodically calibrated and its absolute accuracy found to be $\pm1\%$. The spectra were compiled by a Victoreen Instrument Company 400-channel pulse-height analyzer and recorded on punched paper tape. Corrections to the analyzer spectra for count loss during the analyzer dead time were accomplished by counting into a fast scaler the total number of pulses to the analyzer input and separately the total number of pulses being sorted by the analyzer. Typical spectra are shown in Fig. 1.

For the lighter targets, where inelastic particle groups could be resolved from background, corrections were made to the differential cross sections due to the inelastic groups unresolved from the elastic peak. This was accomplished by averaging the areas under the resolved inelastic groups and then subtracting from the elastic peak the average number of counts per resolved group times the number of unresolved groups. Use was made of the energy level diagrams of these nuclei as published in the *Nuclear Data Sheets*. At the backward angles, estimated errors associated with this subtraction account for the major source of the error flags on the experimental points. For the majority of the spectra the discrete inelastic particle groups could not be resolved from background in the vicinity of the elastic peak. Corrections for this background were made by a linear extrapolation of the background projected under the elastic peak.

Figure 2 contains the measured cross sections as a function of center-of-mass scattering angle. The error flags associated with the experimental points are

[4] H. E. Wegner and W. S. Hall, Rev. Sci. Instr. **29**, 1100 (1958).

determined from counting statistics, charge integration, angle and solid-angle uncertainties, and errors associated with our inability to resolve low-lying excited-state groups from the ground-state group. The ordinates of the curves, the measured differential cross sections, have an additional uncertainty of $\pm 10\%$ due to un-

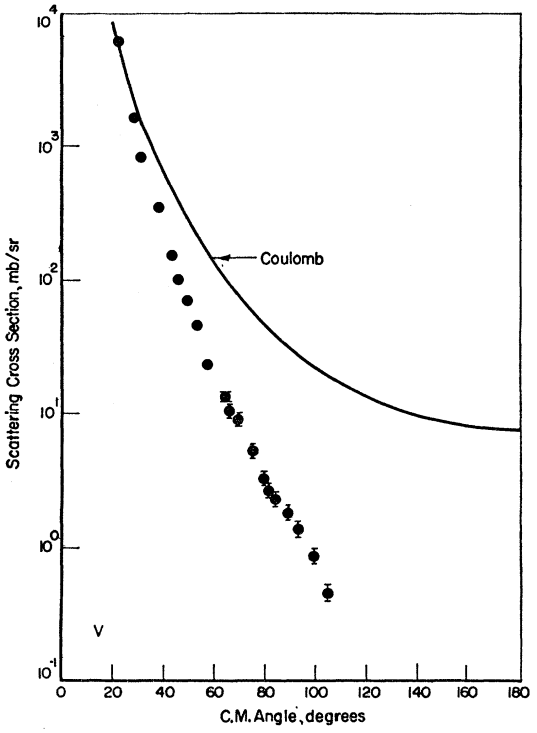

(a)

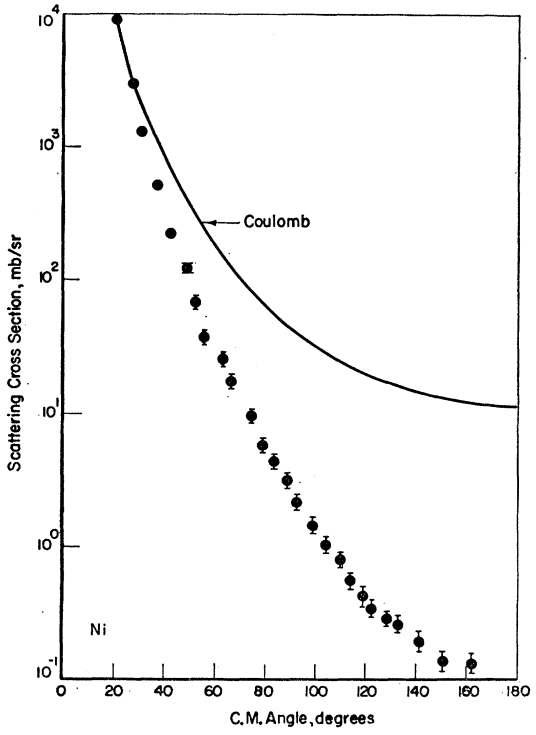

(b)

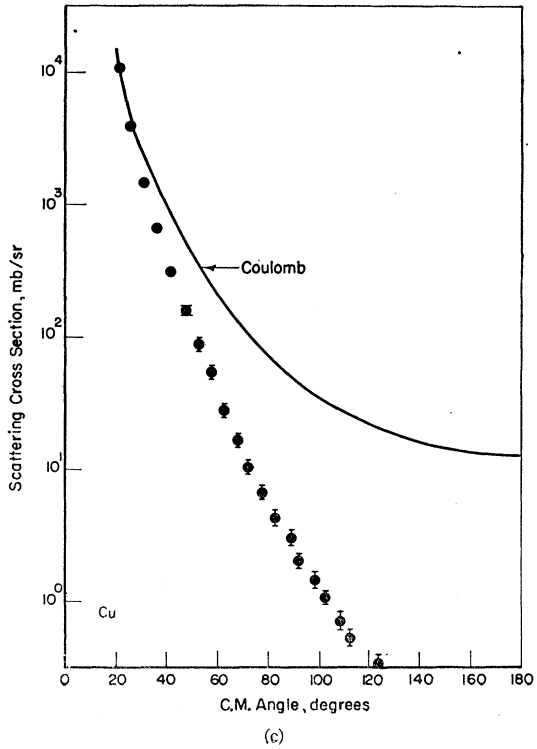

(c)

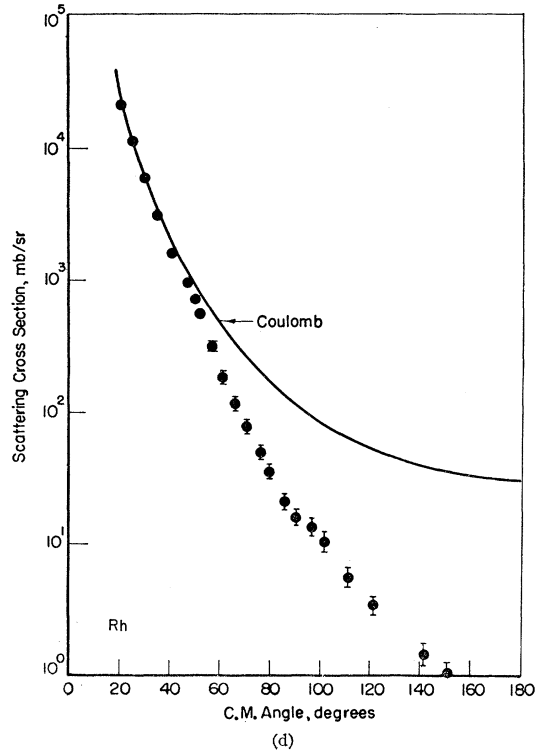

(d)

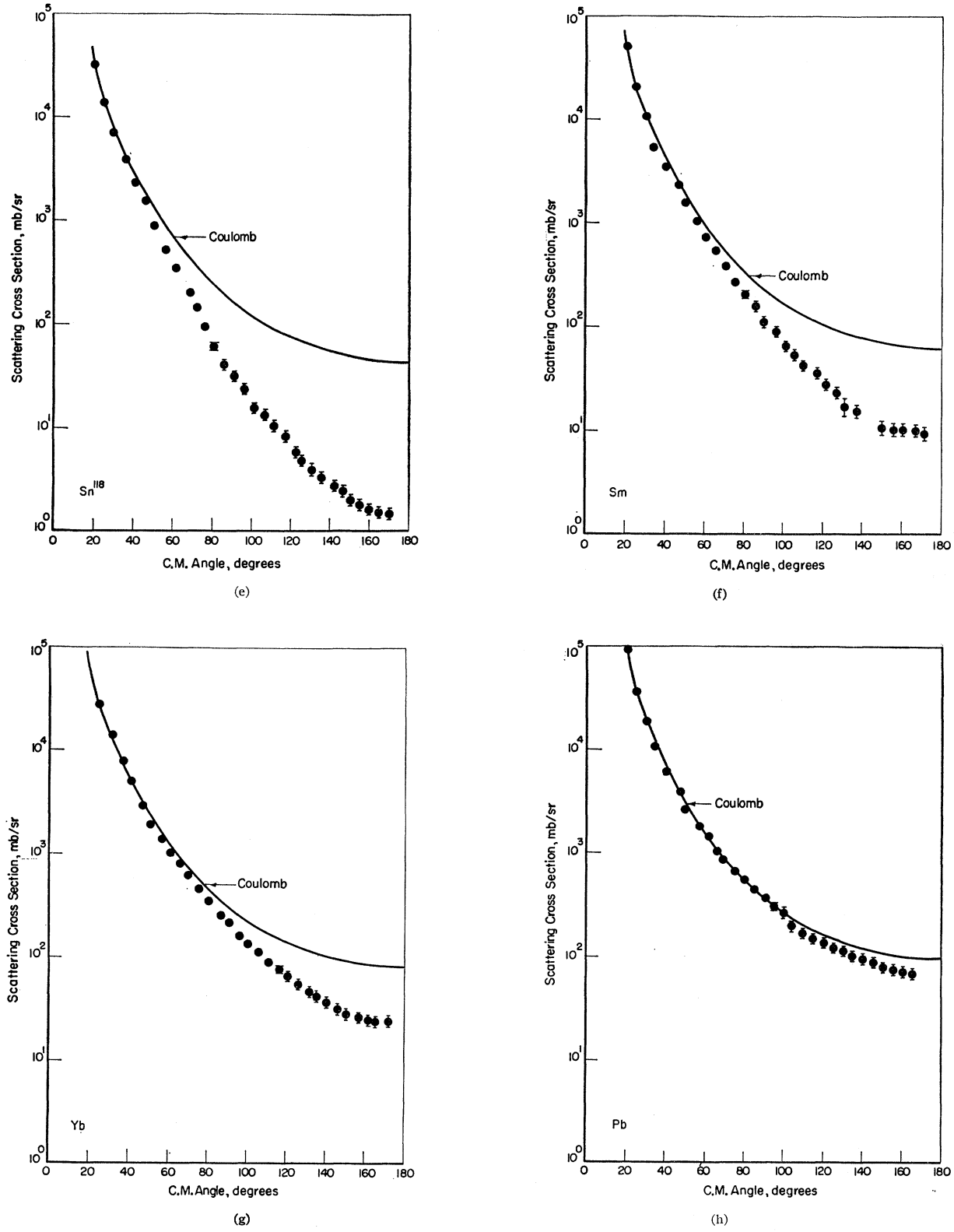

FIG. 2. Angular distributions of the absolute elastic cross section for the scattering of He^3 by (a) vanadium, (b) nickel, (c) copper, (d) rhodium, (e) tin^{118}, (f) samarium, (g) ytterbium, and (h) lead.

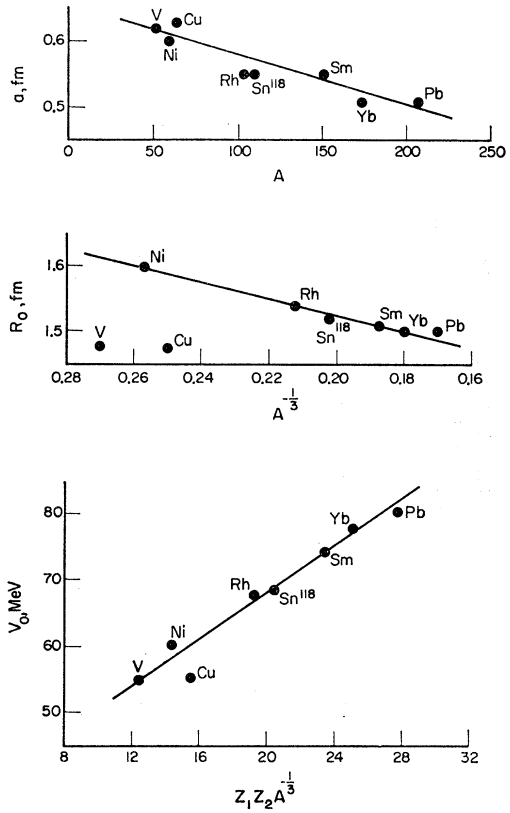

FIG. 3. Plots of mass number (A) versus diffusivity parameter (a), nuclear radius parameter (R_0) versus $A^{-1/3}$, depth of the real part (V_0) of the optical potential versus $Z_1Z_2\,A^{-1/3}$ for the elastic scattering of 20-MeV He^3. The optical-model parameters are those of Trend A given in Table II.

certainties in target thickness determinations. Since the target thickness errors are common to all of the measurements at various angles, the target thickness error flags were not placed on each experimental point. Target thicknesses were determined by weighing the foils and, hence, were a measure of the average target thickness. The estimate of $\pm 10\%$ target thickness uncertainty was not due to weighing errors but rather to estimates of target nonuniformities. Target uniformity was studied[5] by measuring the energy lost in the foils by a collimated beam of alpha particles from a Ra^{228} source.[6] The targets were scanned over a wide region and the estimate of $\pm 10\%$ target thickness uncertainty was associated with the energy-loss variation.

ANALYSIS OF THE EXPERIMENTAL DATA

An optical-model analysis of the experimental data was made using the HUNTER computer code of Drisko and Bassel.[7] The HUNTER code combines an optical-model calculation of differential elastic scattering cross sections and the associated elastic-to-Coulomb ratios with an automatic search of the optical potential parameters. Gross agreement between the calculated cross sections and the corresponding experimental data is indicated by a chi-square (χ^2) test.

The analysis carried out in this experiment considered an optical potential of the Woods-Saxon form with a Thomas-type spin-orbit interaction:

$$V_I=(V_0+iW_0)[1+e^{(r-R)/a}]^{-1}+\left[\frac{\hbar}{M_\pi C}\right]^2 V_s\boldsymbol{\sigma}\cdot\mathbf{L}\frac{1}{r}\frac{d}{dr}[1+e^{(r-R)/a}]^{-1}+V_c.$$

V_0 = real part of the central nuclear potential.
W_0 = imaginary part of the central nuclear potential.
$R=R_0A^{1/3}\times 10^{-13}$ cm, the nuclear radius.
a = nuclear surface diffusivity parameter.
V_s = real part of the nuclear spin-orbit potential.
$\boldsymbol{\sigma}$ = Pauli spin matrix.
$\mathbf{L}$ = orbital angular momentum of the incident particle.
V_c = Coulomb potential:

$$V_c=Z_1Z_2\epsilon^2/2R'[3-(r/R')]^2, \quad r\leq R'$$
$$V_c=Z_1Z_2\epsilon^2/r, \quad r\geq R'$$

$R'=R_cA^{1/3}\times 10^{-13}$ cm, the charge radius.
M = Pion rest mass so that $\hbar/M_\pi C^2=2\times 10^{-26}$ cm^2.

The calculations for this analysis were done at Oak Ridge, Tennessee on the Union Carbide Central Data Processing Facility IBM-7090 digital computer. The initial set of parameters chosen was that obtained by Bassel[8] from an analysis of the 30-MeV He^3 elastic scattering data of Greenlees *et al.*[1,2] The parameters represent the average optimum set for V, Ni, and Cu and will henceforth be referred to as the average 30-MeV parameters.

The calculations were relatively insensitive to the values of V_s and R_c. Therefore, in all but a few special cases, V_s was held fixed at 8 MeV and R_c was held fixed at 1.3 F for V, Ni, Cu, Rh, Sn^{118}, and Sm, 1.4 F for Yb, and 1.5 F for Pb. In all cases a maximum of 20 partial waves was sufficient.

After the first few searches had been made, it was found that the experimental points for nickel, copper, and lead all were significantly displaced from the calculated curves, indicating a possible error in the absolute normalization of the measured cross sections. A similar but smaller displacement was noted in the tin-118, samarium, and ytterbium data. Included in the HUNTER program is the calculation of a multiplicative factor to correct for this displacement. By multiplying the measured cross sections by the calculated

[5] W. S. Steiner, thesis, The Ohio State University, 1963 (unpublished).
[6] E. Bleuler and G. J. Goldsmith, *Experimental Nucleonics* (Holt, Rinehart, and Winston, Inc., New York, 1952).
[7] R. Drisko and R. H. Bassel, Oak Ridge National Laboratory, Oak Ridge, Tennessee (unpublished).
[8] R. H. Bassel, Oak Ridge National Laboratory, Oak Ridge, Tennessee (private communication).

displacement-correction factor, the value of χ^2 is minimized without affecting the shape of the distribution. Values of the displacement correction factor for each of the targets are given in Table I. The correction factors for the Ni, Cu, and Pb targets are outside the $\pm 10\%$ average thickness measurement error. This is attributed to the poor quality of these targets. The Ni target was obtained from a piece of rolled foil and had an uneven surface. The Cu target is of poor texture containing many visible pin holes. The Pb target has an Al backing of unknown surface texture.

During the analysis many searches were conducted. As a result several sets of parameters were obtained for each element. In many cases the value of χ^2 was relatively small though not absolutely minimized. Following the suggestion of Bjorklund *et al.*[9] that the real part of the nuclear potential is a function of Z_1, Z_2 and mass number A through the relation $V_0=K_1+K_2Z_1Z_2A^{-1/3}$, the various values of V_0 were plotted against $Z_1Z_2A^{-1/3}$.

The nuclear radius is defined for the Woods-Saxon form factor as $R=R_0A^{1/3}$. Several studies[10–12] have indicated that good fits to experimental data can be obtained if the nuclear radius is defined as

$$R=C_1A^{1/3}+C_2=(C_1+C_2A^{-1/3})A^{1/3}.$$

This suggests that the nuclear radius parameter depends upon A through the relation

$$R_0=C_1+C_2A^{-1/3}.$$

Consequently, R_0 was plotted against $A^{-1/3}$.

Values of the diffusivity parameter a showed a tendency to decrease with increasing mass number. This effect can be loosely attributed to the increasing Coulomb barrier resulting in a lower effective incident particle energy. As a result the target nucleus shows a greater reflection coefficient by means of a smaller diffusivity parameter. To illustrate this decreasing tendency, a was plotted against the target mass number, A.

By correlating the best curves through the spread of data it was possible to establish two distinct trends:

$$\text{Trend } A \quad \begin{aligned} V_0&=33+1.75\,Z_1Z_2A^{-1/3};\\ R_0&=1.27+1.25\,A^{-1/3};\\ a&=0.658-0.0008\,A; \end{aligned}$$

$$\text{Trend } B \quad \begin{aligned} V_0&=27+1.97\,Z_1Z_2A^{-1/3};\\ R_0&=1.47+0.2\,A^{-1/3};\\ a&=0.658-0.0008\,A. \end{aligned}$$

No correlation could be found for the imaginary part of the nuclear potential, W_0. The only difference between the two trends is in the vanadium, rhodium, and tin parameters. The optimum parameters associated with each trend are listed in Table II. The plots of V_0 against $Z_1\,Z_2\,A^{-\frac{1}{3}}$, R_0 against $A^{-\frac{1}{3}}$, and a against A are given in Figs. 3 and 4.

The establishment by Bassel of an average set of parameters for 30-MeV He^3 elastic scattering from

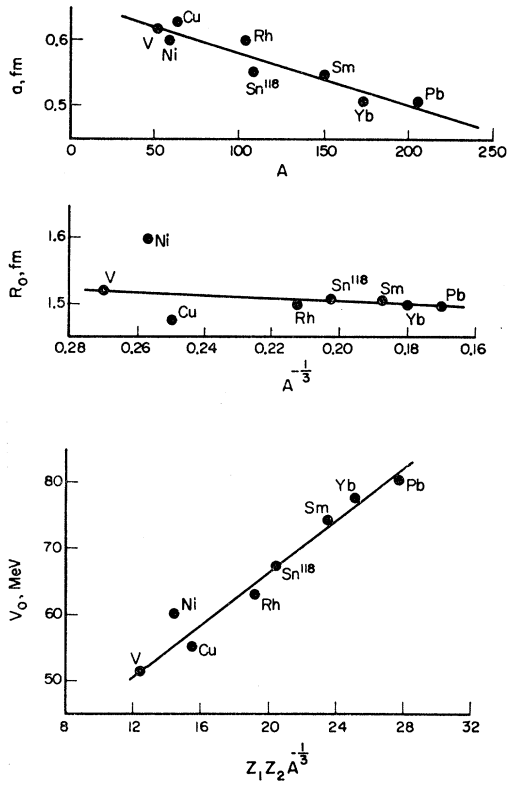

FIG. 4. Plots of mass number (A) versus diffusivity parameter (a), nuclear radius parameter (R_0) versus $A^{-1/3}$, depth of the real part (V_0) of the optical potential versus $Z_1Z_2\,A^{-1/3}$ for the elastic scattering of 20-MeV He^3. The optical-model parameters are those of Trend B given in Table II.

TABLE II. Optimum parameters for trends A and B.

		V_0 (MeV)	W_0 (MeV)	R_0 (F)	a (F)	R_c (F)	V_s (MeV)	χ^2
A	V	54.8	11.9	1.48	0.62	1.3	8	46.1
	Ni	60.1	23.5	1.60	0.60	1.3	8	41
	Cu	55.2	16.4	1.48	0.63	1.3	8	31
	Rh	67.8	14.2	1.54	0.55	1.3	8	70.3
	Sn	68.5	14.4	1.52	0.55	1.3	8	27.9
	Sm	74.4	47.6	1.51	0.55	1.3	8	32
	Yb	77.1	10.0	1.50	0.51	1.4	8	41.1
	Pb	80.5	1.7	1.50	0.51	1.5	8	4.1
B	V	51.6	13.4	1.52	0.62	1.3	8	59.8
	Ni	60.1	23.5	1.60	0.60	1.3	8	41
	Cu	55.2	16.4	1.48	0.63	1.3	8	31
	Rh	63.1	27.7	1.50	0.60	1.3	8	62.6
	Sn	67.6	13.8	1.51	0.55	1.3	8	27.9
	Sm	74.4	47.6	1.51	0.55	1.3	8	32
	Yb	77.1	10.0	1.50	0.51	1.4	8	41.1
	Pb	80.5	1.7	1.50	0.51	1.5	8	4.1

[9] F. E. Bjorklund, G. Campbell, and S. Fernbach, Proceedings of the International Symposium on Polarization Phenomena of Nucleons, Basel, 1961 (unpublished).

[10] M. A. Melkanoff, J. S. Nodvick, D. S. Saxon, and R. O. Woods, Phys. Rev. **106**, 1319 (1957).

[11] J. R. Beyster, M. Walt, and E. W. Salmi, Phys. Rev. **106**, 1319 (1957).

[12] G. Igo and R. M. Thaler, Phys. Rev. **106**, 126 (1957).

TABLE III. Average optical-model parameters for vanadium, nickel, and copper at 20 and 30 MeV.

	20 MeV	30 MeV[a]
V_0 (MeV)	55.0	68.1
W_0 (MeV)	14.6	14.4
a (F)	0.62	0.61
R_0 (F)	1.48	1.51
R_c (F)	1.3	1.3
V_s (MeV)	8	8

[a] See Ref. 8.

vanadium, nickel, and copper suggests that average parameters for these elements may exist for 20-MeV scattering. The best parameters obtained in the present analysis for vanadium and copper do not differ greatly and were therefore averaged to give a single set. These parameters are referred to as the average 20-MeV parameters. Table III lists the average 20-MeV parameters obtained in this analysis and the average 30-MeV parameters of Bassel. Good fits to the vana-

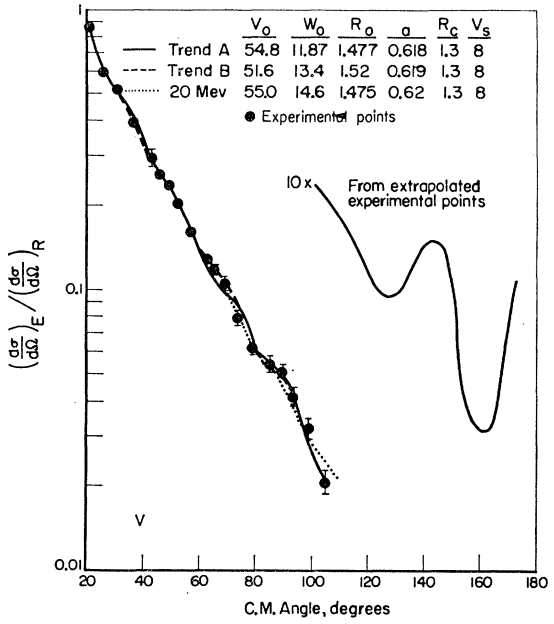

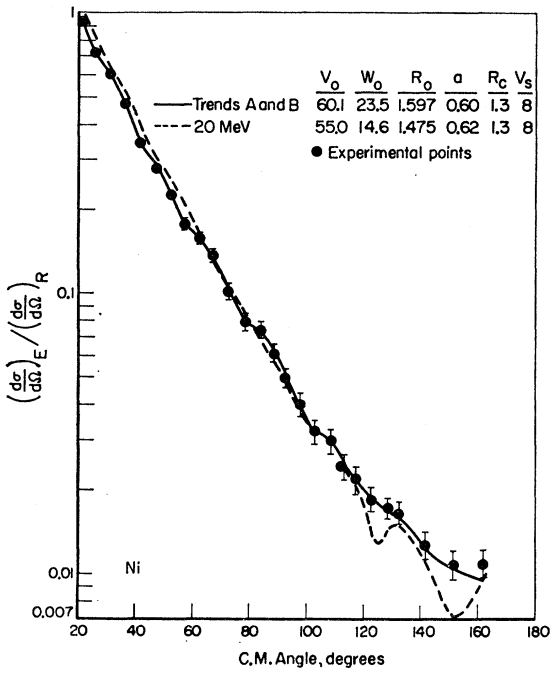

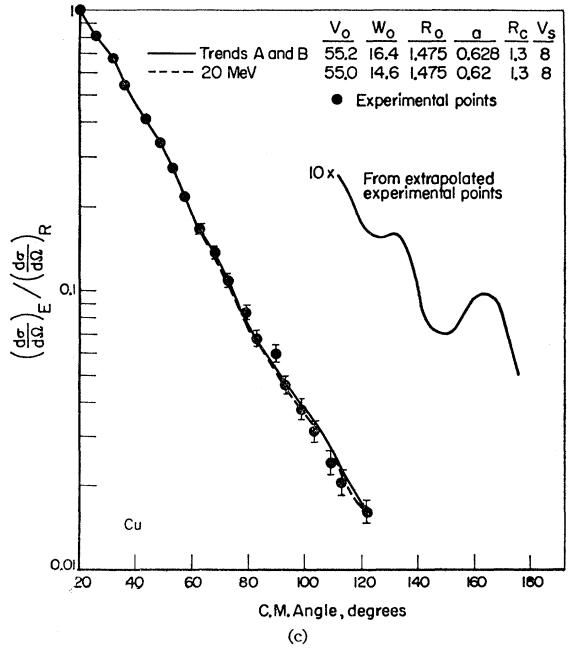

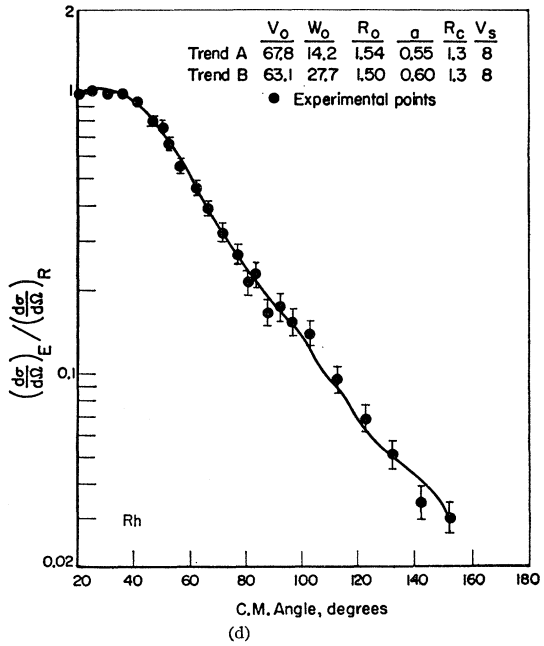

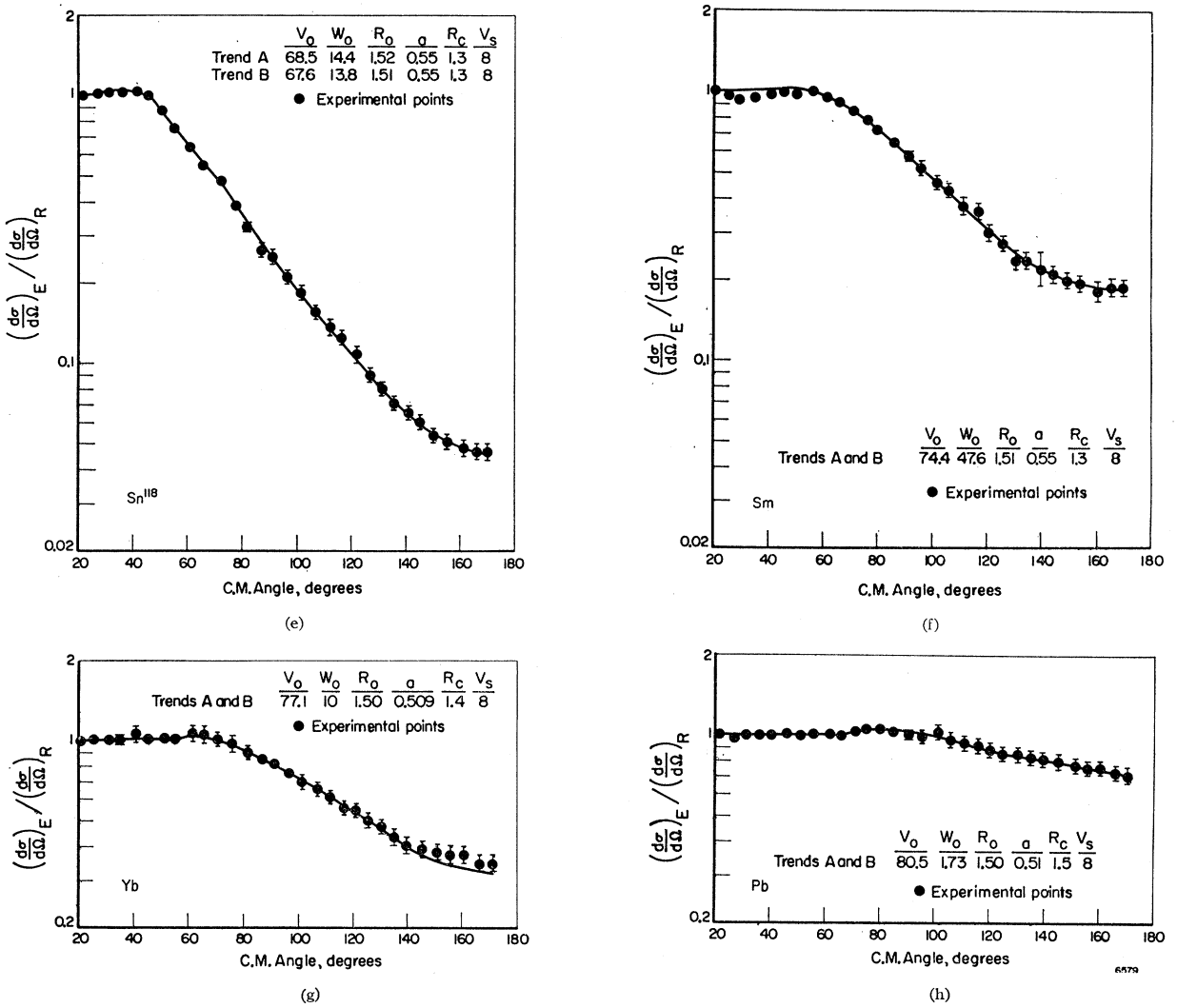

FIG. 5. Angular distributions of the elastic-to-Coulomb cross-section ratio for the scattering of He^3 by (a) vanadium, (b) nickel, (c) copper, (d) rhodium, (e) tin^{118}, (f) samarium, (g) ytterbium, (h) lead. The smooth curves represent the distributions given by the optimum parameters as determined using the HUNTER search code.

dium and copper data are obtained using the average 20-MeV parameters. However, the experimental data extend only to 110 deg. The nickel data, which extend to 170 deg, are fit equally well up to 110 deg, but very poorly beyond 110 deg where the theoretical curve oscillates too vigorously. HUNTER calculations could not be performed for the back angle curves for vanadium and copper. This is because the code is programmed to provide calculations only at angles for which input cross sections are given. In order to obtain an indication of the degree of oscillation in the vanadium and copper angular distribution curves at back angles, HUNTER calculations were forced to 170 deg by providing as input, extrapolations of the experimental data. This was done for only one case and used the average 20-MeV parameters. The resulting curves showed oscillations similar to those of the nickel curve.

Figure 5 contains the theoretical angular distribution curves as obtained from the optimum parameters and the displacement-corrected cross sections. The shapes of the vanadium and copper curves beyond 110 deg as obtained from the forced HUNTER calculations are indicated.

COMPARISON WITH OTHER RESULTS

The average 20-MeV parameters established in the experiment for vanadium, nickel, and copper can be compared to the average 30-MeV parameters established for vanadium, nickel, and copper by Bassel. The real part of the nuclear potential is larger in the 30-MeV case while the radius parameter is smaller. The other parameters are relatively unchanged. However, it must be noted that these parameters are based on experi-

mental data extending to scattering angles no greater than 120 deg.

Extensive optical-model analyses of 30-MeV He^3 scattering data have been done by Hodgson *et al.*[13–15] and Greenlees *et al.*[2] These analyses tend to equalize the values of the real and imaginary parts of the nuclear potential at approximately 30–50 MeV. In the analysis conducted for the present experiment, the imaginary part of the potential was held to a value less than that of the real part, the ratio being approximately two or three to one. Consequently, quantitative comparison with the Hodgson results cannot be readily made.

CONCLUSIONS

Departures from Coulomb scattering have been observed in the elastic scattering of 20-MeV He^3 particles from V, Ni, Cu, Rh, Sn^{118}, Sm, Yb, and Pb. Diffraction-like oscillations in the elastic-to-Coulomb cross-section ratio are evident, although not pronounced, in the lighter element data.

The optical-model analysis carried out in the experiment considered only a Woods-Saxon-type potential with a Thomas-type spin-orbit interaction. In this regard the analysis cannot be considered exhaustive even though reasonable fits to the data are obtained and trends among the parameters noted.

Experimental data for vanadium and copper were obtained at scattering angles extending only to 110 deg. An average set of parameters was established which gives good fits to these data. The same set of parameters gives a good fit to the nickel data up to 110 deg, but gives an angular distribution for the cross section which oscillates too vigorously beyond 110 deg. By providing extrapolated input data to the HUNTER program, calculations of the back-angle cross sections for vanadium and copper using the average 20-MeV parameters were obtained. Oscillations similar to those for nickel were indicated.

The relatively small oscillations in the observed nickel cross sections suggest that only small oscillations may exist in the vanadium and copper cross sections. Consequently, the average 20-MeV parameters established in this experiment and the average 30-MeV parameters established by Bassel may not provide a good fit to the data at back angles. In this regard, an interesting extension of both the present experiment and the 30-MeV experiment would be the investigation of back-angle elastic scattering for elements below copper.

The results obtained for the heavy elements show a smooth and gradual departure from Coulomb scattering at large angles. As a result, equally good fits to the data are obtained with a wide choice of parameters. In order to unambiguously define the parameters, additional data are needed. Analysis of reaction cross sections provides a means of determining the nuclear absorption, and hence, leads to values for W_0 as well as defining the form factors. In addition, polarization studies are needed to establish the form of the spin-orbit potential.

ACKNOWLEDGMENTS

The authors wish to acknowledge the excellent and continued assistance provided by the staffs of The Ohio State University Cyclotron Laboratory and Electrostatic Generator Laboratory. One of us (R. W. K.) is indebted to Battelle Memorial Institute for the Battelle Staff Fellowship given in support of this research.

In addition we are indebted to Dr. R. H. Bassel of the Oak Ridge National Laboratory for his continued interest in this work and his guidance in the analysis of the experiment. Particular acknowledgment is given Dr. Bassel for providing both the results of his 30-MeV analysis and use of the HUNTER program prior to publication.

Gratitude is expressed to the Oak Ridge National Laboratory for the hospitality and cooperation extended in the use of the computer and other analytical facilities.

[13] P. E. Hodgson, Nucl. Phys. **21**, 28 (1960).
[14] P. E. Hodgson, Nucl. Phys. **23**, 499 (1961).
[15] J. Aguilar, A. Garcia, J. B. S. England, P. E. Hodgson, and W. T. Toner, Nucl. Phys. **25**, 259 (1961).